



Climate-change impact on reservoir evaporation and water availability in a tropical sub-humid region, north-eastern Brazil

Gláuber P. Rodrigues^{1,2}, Arlena Brosinsky^{2,3}, Ítalo S. Rodrigues⁴, George L. Mamede⁵, José C. de Araújo¹

¹ Department of Agricultural Engineering, Federal University of Ceará, 60451-070 Fortaleza, Brazil

5 ² Institute for Environmental Sciences and Geography, University of Potsdam, Potsdam, Germany

³ Remote Sensing and Geoinformatics Section, German Research Centre for Geosciences (GFZ), Potsdam, Germany

⁴ Department of Geography, University of Lethbridge, Lethbridge, Alberta, Canada

⁵ Institute for Engineering and Sustainable Development, University of International Afro-Brazilian Integration, 62.790-000 Redenção, Brazil.

10 *Correspondence to:* Gláuber P. Rodrigues (pontesglauber@gmail.com)

Abstract. The potential effects of climatic changes on water resources are crucial to be assessed, particularly in dry regions such as Northeast Brazil (1 million km²), where water supply is highly reliant on open-water reservoirs. This study analyses the impact of evaporation (by the Penman method) on water availability for four scenarios based on two regional climatic models (Eta-CanESM2 and Eta-MIROC5) under the Representative Concentration Pathways 4.5 and 8.5. We compared the water availability in the period of 2071-2100 with that of the historical period (1961-2005). The scenarios derived from the Eta-CanESM2 model indicate an increase in dry season evaporative rate (2% and 6%, respectively) by the end of the century. Unlike the above scenarios, the ones derived from the Eta-MIROC5 model both show a decrease in dry season evaporative rate of -2%. Consequently, for a 90% reliability level, the expected reservoir capacity to supply water with high reliability is reduced in 80%. It is reasonable to state that both patterns of future evaporation in the reservoirs may prove to be plausible. Because model-based projections of climate impact on water resources can be quite divergent, it is necessary to develop adaptations that do not need quantitative projections of changes in hydrological variables, but rather ranges of projected values. Our analysis shows how open water reservoirs might be impacted by climate change in dry regions. These findings complement a body of knowledge on estimation of water availability in a changing climate and provide new data and insights on water management in reservoir-dependent drylands.

25 1 Introduction

The increasing atmospheric concentration of greenhouse gases is changing the Earth's climate more rapidly than ever before (Konapala et al., 2020). Expected changes in climate variables, such as rainfall and temperature, may result in alterations in the hydrological cycle and, thus, the necessity of adaptations of current reservoir management strategies (Minville et al. 2010). As climate changes, it is imperative to identify its impact on water supply, especially with respect to open-water reservoirs located in drylands.



As stated by Adrian et al. (2009), lakes, reservoirs and other inland open-water surfaces are likely to serve as good sentinels for current climate change because (1) aquatic ecosystems are well defined and are studied in a continuous way; (2) they respond directly to climate change and also incorporate the effects of climate-driven changes occurring within the catchment; (3) they integrate responses over time, which can filter out random noise; and (4) they are distributed worldwide and, as such, can act as sentinels in many different geographic locations and climatic regions, capturing different aspects of climate change (e.g., rising temperature, glacier retreats, permafrost melting). Indeed, several investigations worldwide have highlighted the impact of climate change on water resources. Reservoirs are essential infrastructures for the economic and social development of the region, and their evaporation losses are significant for the water system and can severely impact water availability and allocation (Malveira et al., 2012; Mamede et al., 2012; Peter et al., 2014).

In hydrology and in studies relating to water availability, free-surface evaporation plays an important role. However, despite numerous approaches developed over the last 200 years to estimate evaporation (McMahon et al., 2016), there are still uncertainties within concerning evaporation assessment, and the main reasons for this are: the high cost of maintaining the equipment (including personnel training); the numerous parameters needed to apply the equations; and the use of databases located far from the respective water bodies (for instance, class-A pans or meteorological stations). Additionally, remote sensing tools can assist in monitoring evaporation (Cui et al., 2019) and water volume loss in general (Zhang et al., 2021). As stated by (Su, 2002), conventional techniques that employ point measurements to estimate the components of energy balance are representative only of local scales and cannot be extended to large areas because of the heterogeneity of land surfaces and the dynamic nature of heat transfer processes. Remote sensing is probably the only technique which can provide representative measurements of several relevant physical parameters at scales from a point to a continent. Techniques using remote sensing information to estimate atmospheric turbulent fluxes are therefore essential when dealing with processes that cannot be represented by point measurements only.

Climate change plays a critical role in the planning of water resources: the water cycle is expected to be accelerated because of temperature increase; in warm climates, climate change is expected to worsen water shortage episodes. Investigations show the sensitivity of inland water bodies as physical, chemical, and biological water properties respond rapidly to climate-related changes (Adrian et al., 2009; Rosenzweig et al. 2007). Climate change is studied using global circulation models, usually with a coarse spatial resolution of hundreds of kilometres, disregarding regional factors in the process of modelling (Chou et al., 2014; Navarro-Racines et al., 2020). Hence, the importance of regional climate models (RCMs), which have a smaller scale (usually tens of kilometres) and consider local factors such as topography, land cover, and land use. One of the issues addressed refers to the resilience of metropolitan areas to climate change, where major problems may be related to rapid changes in water supply, among others (Lyra et al., 2018).

The Metropolitan Region of Fortaleza (MRF) has a population of over 4 million inhabitants (IBGE, 2022), one of the most densely populated areas in Brazil. Its water supply is highly dependent on an extensive network of open-water reservoirs, almost entirely located in the semiarid region (Mamede et al., 2018; Peter et al., 2014). Despite the well-known sensitivity of dry regions to changes in climate, little is yet known about the impacts on water resources in this region and how water

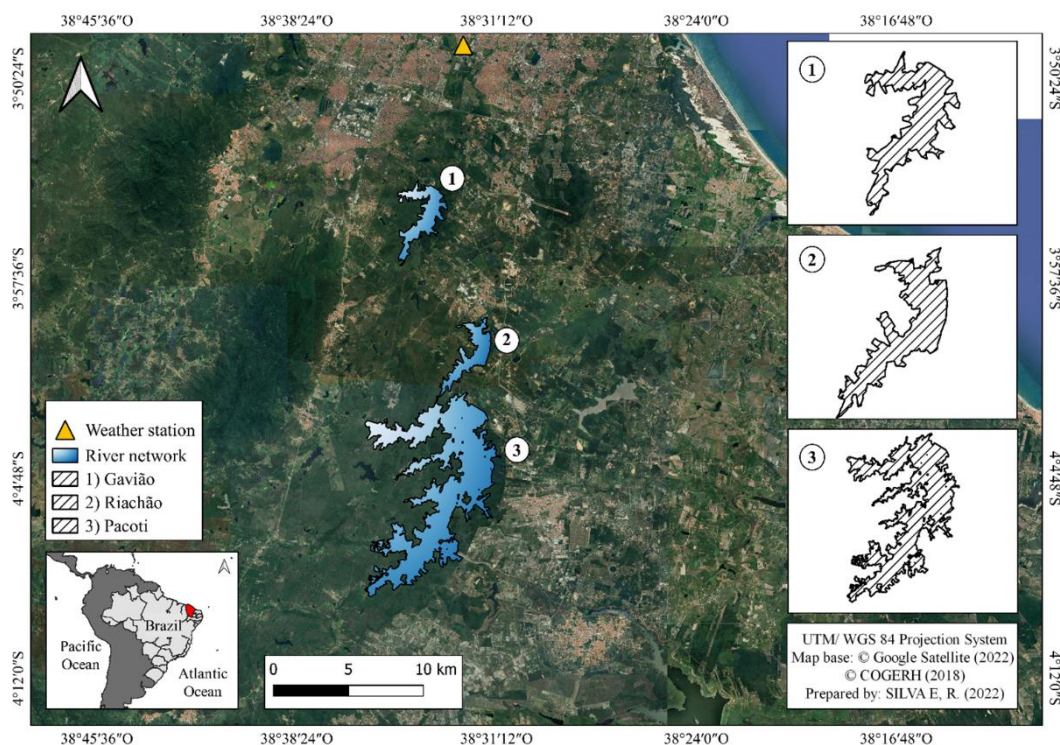


65 availability may be affected by climate change. With this investigation, we intend to increase the amount of information
currently existing on the potential impacts of climate change on water resources in Northeast Brazil. After several studies in
this region have focused on temperature variation (Marengo et al., 2009) and precipitation (Almagro et al., 2020), our analysis
will contribute to the growing body of knowledge on surface water reservoirs and how they respond to climate change.
More specifically, the objective of this research was to analyse the impact of climate change on reservoir evaporation and
70 consequently on water availability in the MRF, a densely populated urban area located in North-eastern Brazil. To achieve this
goal, we (i) assessed historical and present evaporation by means of a weather station and remote sensing calculations, (ii)
compared them to historical and future simulations based on four climate change scenarios, and (iii) investigated the impact
of evaporation change on water availability using stochastic modelling.

75 **2 Study area**

The state of Ceará is situated in the north-eastern region of Brazil (Figure 1), mostly semiarid (BSh, according to Köppen
classification), a dryland where various studies on the impacts of climate change have shown susceptibility to severe climate
extremes, more prominently droughts (Alvalá et al., 2019; Marengo et al., 2017, 2022; Vieira et al., 2020). The average annual
80 rainfall in the region ranges from 500 to 800 mm (of which 80% occurs between January and April) and the average annual
temperature is 26 °C (INMET, 2019; Rodrigues et al., 2021a). This region has high water vulnerability resulting from irregular
rainfall associated with ephemeral rivers, high potential evaporation rates exceeding 2000 mm per year, and shallow soils over
crystalline basement (de Araújo and Piedra, 2009; Medeiros and de Araújo, 2014). This soil-feature allows limited storage of
water (Alvalá et al., 2019), which when present is often salty because of the prevalence of fissural aquifers in crystalline
bedrock.

85 The reservoirs studied in this research are located in a tropical-coastal area whose climate is slightly different from the
predominant semi-arid condition described above (rainfall of 1,600 mm year⁻¹ and relative humidity of 78%) – however, they
are supplied by a water system from the drylands.



90 **Figure 1: Location of the state of Ceará (bottom left) and the major reservoirs that supply the Metropolitan Region of Fortaleza, the hydrographic network, and the INMET (Brazilian National Institute of Meteorology) weather station. Daily meteorological observed variables from the station were used spanning 1961 to 2005.**

The reservoirs under analysis (Pacoti, Riachão and Gavião, see Table 1 and Figure 1) are responsible for supplying water to the 4.2 million inhabitants of the MRF region, and comprise the downstream sector of a network of reservoirs located in the sub-humid area. Unlike the reservoirs that supply them, the water level of the three reservoirs does not decrease substantially during the dry season, due to a transposition system that provides water.

Table 1: Technical characteristics of Pacoti, Riachão, and Gavião reservoirs.

	Pacoti	Riachão	Gavião
Storage capacity (hm ³)	380.0	47.9	33.3
Catchment area (km ²)	1,110	34	97
Hydraulic basin (km ²)	37.0	5.7	6.2

Source: Ceará State Secretariat for Water Resources, SRH (2015).



3 Methodology

105 We used the regional Eta model (Mesinger et al. 2012) nested to two Global Circulation Models (CanESM-2 and MIROC5) at Representative Concentration Pathways 4.5 and 8.5. The investigation was performed in three phases: the first consisted of the simulation of regional evaporation pattern with bias correction; the second consisted of the combined application of remote sensing and on-site measurement to assess open-water evaporation; and on the third, we analysed the impact of evaporation changes on water availability for four scenarios. For ease and convenience, the four scenarios are hereafter referred to as C4 (model Eta-CanESM2, Pathway 4.5), C8 (model Eta-CanESM2, Pathway 8.5), M4 (model Eta-MIROC5, Pathway 4.5), and M8 (model Eta-MIROC5, Pathway 8.5). The methodological framework is presented in Figure 2. All climate projections set time slices as follows: historical (1961-2005), near term (2006-2040), midterm (2041-2070), and long term (2071-2099).

110

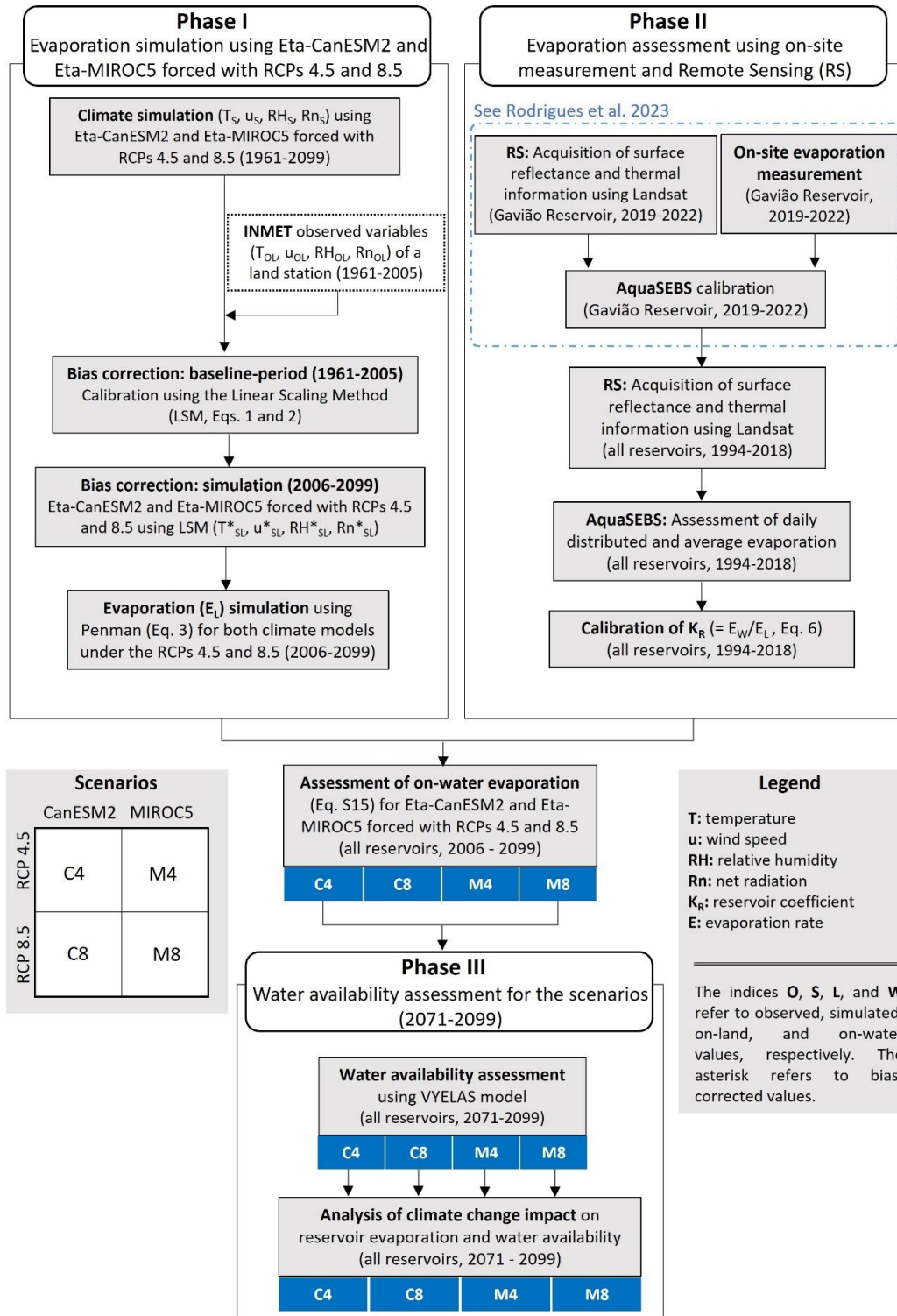


Figure 2: Methodological flowchart for the simulation of evaporation with climate models and assessment of water availability.



3.1 Phase I: Evaporation simulation forced with RCPs 4.5 and 8.5

115 Using the regional model Eta (Mesinger et al. 2012), from the Brazilian National Institute for Space Research (INPE), we
assessed daily meteorological variables, such as net radiation, wind speed, air temperature, and relative humidity. The Eta
model is nested to the Japanese MIROC5 (The University of Tokyo Centre for Climate System Research, Watanabe et al.,
2010) and to the Canadian CanESM-2 (Canadian Centre for Climate Modelling and Analysis, Chylek et al., 2011). According
to Chou et al. (2014), the Brazilian model has been used operationally at INPE since 1997 for weather forecasts, and since
120 2002 for seasonal climate forecasts. The model was set up with a spatial resolution of 20 km, covering both South and Central
Americas.

Since the Fifth Assessment Report (AR5) from the Intergovernmental Panel on Climate Change (IPCC 2014), the greenhouse
gas concentration scenarios are based on the Representative Concentration Pathways (RCP), which are expressed in terms of
radiative forcing toward the end of the twenty-first century. In this study, the downscaled products were simulated based on
125 RCP4.5 and RCP8.5. The first provides a climate forcing that reaches 4.5 W m^{-2} by 2050, with further stabilization; the latter
provides continued growth of the radiative forcing to reach 8.5 W m^{-2} by 2100 (Bjørnæs 2013). All the simulated data were
extracted from the INPE Portal “Climate Change in Brazil” and made available on the PROJETA Platform
(<https://projeta.cptec.inpe.br>).

Outputs from regional climate models are subject to systematic errors (biases), therefore, bias correction is recommended
130 (Graham et al., 2007) for the sake of simulation reliability (Teutschbein and Seibert, 2012). To correct bias, we applied the
Linear Scaling Method (LSM), often used in studies of hydrological impacts of climate change (Althoff et al., 2020; Oliveira
et al., 2017; Fiseha et al., 2014). The correction is based on the identification of biases between observed and simulated climate
variables. Temperature (T) is corrected with an additive factor ($\bar{T}_{\text{obs}} - \bar{T}_{\text{sim}}$, Equation 1, where both terms are the monthly
average), whereas the remaining meteorological variables (represented by the letter C) are corrected with a multiplicative
135 factor ($\bar{C}_{\text{obs}} / \bar{C}_{\text{sim}}$, Equation 2, where both terms are the monthly average).. Equations 1 and 2 were used for both the baseline
(1961-2005) and scenarios simulation (2006-2099) periods.

$$T_{(t)}^* = T_{(t)} + \bar{T}_{\text{obs}} - \bar{T}_{\text{sim}} \quad (1)$$

$$C_{(t)}^* = C_{(t)} \cdot \left(\frac{\bar{C}_{\text{obs}}}{\bar{C}_{\text{sim}}} \right) \quad (2)$$

In Equations 1 and 2, the variables to which C refers are relative humidity (%), wind speed at 2 m height (m s^{-1}), and net
radiation ($\text{MJ m}^{-2} \text{day}^{-1}$); the asterisk indicates the climate variable values after bias correction.



3.2 Phase II: Evaporation assessment using on-site measurement and Remote Sensing

140 3.2.1 On-land (E_L) evaporation assessment

Daily meteorological observed variables from a station of the Brazilian National Institute of Meteorology (INMET) were used for bias correction of the climate model for the period from 1961 to 2005 (station code: 82397 - Fortaleza). The station was chosen due to two aspects: it is the nearest weather station to the reservoirs (15 km away), and it has longer historical series (since 1961) with fewer flaws. To assess on-land evaporation, we used the Penman (1948) Equation 3:

$$E_L = \frac{\Delta}{\Delta + \gamma} \cdot \frac{R_n}{\lambda_V} + \frac{\gamma}{\Delta + \gamma} \cdot f(u) \cdot (e_s - e_a) \quad (3)$$

145 In Equation 3, E_L is the open-water evaporation rate (mm d^{-1}); R_n is the net radiation at the water surface ($\text{MJ m}^{-2} \text{d}^{-1}$); Δ is the slope of the saturation vapour pressure curve ($\text{kPa } ^\circ\text{C}^{-1}$) at air temperature; γ is the psychrometric coefficient (assumed $0.0665 \text{ kPa } ^\circ\text{C}^{-1}$); ρ is the density of water (1000 kg m^{-3}); λ_V is the latent heat of vaporization (assumed 2.5 MJ kg^{-1}), $(e_s - e_a)$ is the difference between saturation and partial water vapour pressure (kPa), and $f(u)$ is a function used to account for the advective drying effects of wind ($\text{mm d}^{-1} \text{kPa}^{-1}$). In Equation 4, u is the wind speed at 2 m height (m s^{-1}). We have adopted the Penman
150 (1956) form of the wind function:

$$f(u) = 1.313 + 1.381 \cdot u \quad (4)$$

A trend analysis was performed using the Mann-Kendall method (Kendall, 1975; Mann, 1945) applied to both the calculated and the simulated Penman-evaporation. The null hypothesis is that there is no trend in the series. The three hypotheses evaluated are: i) no trend, ii) positive trend, iii) negative trend. A significance level of $p = 0.05$ was adopted. The magnitude
155 of the changes was evaluated by the nonparametric Sen's slope and Kendall's tau (τ) coefficient, which describes the relationship between variables.

3.2.2 On-water (EW) evaporation assessment

The on-water evaporation rate was estimated with the remote sensing algorithm AquaSEBS (Surface Energy Balance of Fresh
160 and Saline Waters, see Abdelrady *et al.*, 2016). The algorithm is a modification from Su (2002) and was developed to estimate the heat fluxes by integrating satellite data and hydro-meteorological field data. It has been validated on the study region (Rodrigues *et al.*, 2021a, 2021b), and requires three sets of data as input: (i) remote-sensing data, including emissivity, surface albedo and surface temperature; (ii) meteorological data; and (iii) radiative forcing parameters (Abdelrady *et al.*, 2016), such as downward shortwave and long-wave radiations. For the temporal estimation of evaporation, were used: bands 1 to 5
165 (reflectance) and band 6 (thermal) from Landsat 5 (Thematic Mapper - TM) and bands 1 to 7 (reflectance) and band 10 (thermal) from Landsat 8 (Optical Land Imager - OLI). Due to the technical characteristics of the sensors (radiometric, spectral,



and thermal band spatial resolutions), methodological adjustments were necessary to acquire some parameters in the model application (see Supplementary Material 1).

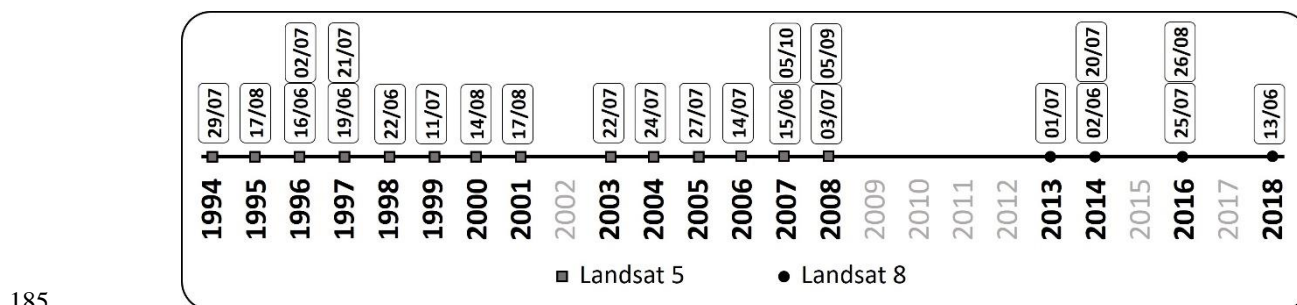
170 AquaSEBS uses energy balance to calculate instantaneous latent heat flux of evaporation (Equation 5), thus, evaporation is calculated for each pixel of the image. The energy balance of the water surface can be expressed as it follows:

$$E_w = \frac{R_n - G_w - H}{\lambda v \cdot \rho} \quad (5)$$

In Equation 5, R_n is net radiation at the water surface, G_w is the water (or ground for land surfaces) heat flux, and H is sensible heat to the air. All terms are expressed in $W m^{-2}$. Detailed information about the algorithm and the meteorological input is in the Supplementary Material 1 of this manuscript. To assess the on-water evaporation rate (E_w) in the scenarios, we used Equation 6, in which E_L is the on-land evaporation rate and K_R is a coefficient. E_L refers to a value provided by the models
 175 Eta-CanESM2 and Eta-MIROC5, whose bias was corrected using data from an on-land meteorological station. The coefficient K_R was calibrated using AquaSEBS to assess E_w and Penman Equation 3 to estimate E_L based on data from the INMET station.

$$E_w = K_R \cdot E_L \quad (6)$$

For calibration purposes, AquaSEBS used images spanning from 1994 to 2018 containing the three studied reservoirs. A total of 24 scenes were used, eighteen from Landsat 5 and six from Landsat 8 (Figure 3), all acquired from the United States Geological Survey portal (<https://earthexplorer.usgs.gov/>, last accessed 09/08/2022). We used images exclusively from the
 180 dry season (June to December) due to the following reasons: (i) cloud-free images are easier to obtain in these months; (ii) the water-availability model (Phase III) only considers evaporation of the dry period; and (iii) this is the period when evaporation is more intense and, thus, more relevant to water management purposes.



185 **Figure 3: Temporal distribution of Landsat images used to assess on-water evaporation with the AquaSEBS algorithm and, thus, to calibrate the K_R coefficient. Years shown in grey did not have cloud-free images**

3.3 Phase III: Water availability assessment for the scenarios in the long-term future (2071-2099)

190



The VYELAS model (Volume-Yield-Elasticity, as in de Araújo *et al.*, 2006) was applied to simulate water availability. River inflow to the reservoir is generated by a stochastic procedure, using the inverse of the two-parameter gamma probability density function (see McMahon and Mein, 1986; and Campos, 1996). The parameters of the distribution were derived from the average and standard deviation of historical annual inflow to the reservoir. A 10,000-year synthetic series was generated for each of the three reservoirs, which reproduced the historical average and the coefficient of variation of annual inflow as given in Table 2. VYELAS simulates the reservoir water balance for a large synthetic series, corresponding to the number of annual water-balance simulations (Equation 7). Each set of simulations is associated with a withdrawal discharge (Q_w). The model calculates the annual reliability level (G), which corresponds to the annual probability of providing the target withdrawal discharge and is given by $G = 1 - N_s/N$, where N_s is the number of successful years and N the total number of years in the simulation (Campos, 2010; McMahon and Mein, 1986). In this context, a successful year is one in which the target water withdrawal can be integrally met without leading the reservoir reserve below the minimum operational volume (de Araújo *et al.*, 2018). Campos (2010) states that the water balance of reservoirs in semiarid environments is approximately:

$$\frac{\Delta V}{\Delta t} \approx Q_{in} - Q_{E, dry} - Q_s - Q_w \quad (7)$$

In Equation 7, V is the water storage volume in the reservoir, t represents time, Q_{in} the inflow from the river network into the reservoir, $Q_{E, dry}$ the water loss due to evaporation in the dry season, Q_s the reservoir outflow over the spillway, and Q_w the water withdrawal from the reservoir (all variables in $hm^3 \text{ year}^{-1}$). The model assumes that water input by rainfall directly onto the reservoir surface, together with groundwater discharge into the reservoir, is compensated by wet season evaporation and outflow due to seepage. VYELAS demands data of seasonal water inflow (average and standard deviation), precipitation, evaporation, storage capacity (SC), alert volume, and the morphological parameter α ($SC = \alpha \cdot y^3$, where y is the water maximum depth) (Campos, 2010).

The evaporation rates simulated for the long-term future (last 30 years of the century) of the two models were adjusted by the K_R coefficient (see Equation 6) and used as input in the VYELAS model. The input data required to run the model are listed in Table 2.

Table 2. Input data for the VYELAS model for the three reservoirs.

	Gavião	Riachão	Pacoti
Average inflow ($hm^3 \text{ yr}^{-1}$) ^a	32.6	7.8	254.5
Coefficient of variation annual inflow ^b	0.8	0.8	0.8
Reservoir-shape coefficient ^c	17927	5007	31174
Evaporation in the dry season ($m \text{ yr}^{-1}$) ^d	1.3	1.3	1.3
Maximum storage capacity (hm^3) ^a	33.3	47.9	380.0
Minimum operational volume (hm^3) [*]	5.0	7.2	57.0



Initial volume in the first simulation year (hm ³)**	16.3	3.9	127.2
--	------	-----	-------

Source of data: ^aCOGERH (2020); ^bMacêdo (1981); ^cFeitosa et al. (2021); ^dCalculated in this study.

*The minimum operational volume was assumed as 15% of the reservoir storage capacity (de Araújo *et al.*, 2018).

**Initial volume is the smallest value between half of maximum storage capacity and half of the annual average inflow (Campos, 2010)

220

To assess how water availability varies with evaporation rate changes, we use the concept of elasticity (ϵ , as in de Araújo et al., 2006; 2018), represented by Equation 8, in which Q_{90} is the water availability with 90% annual reliability and E is the evaporation rate. Therefore, the higher the elasticity, the more significant the impact of evaporation on water availability. The asterisk refers to the reference values.

$$\epsilon(Q_{90}:E) = \frac{\Delta Q_{90}/Q_{90}^*}{\Delta E/E^*} \quad (8)$$

225 The VYELAS model has been used in hydrological studies assessing the effects of water quality on evaporation (Mesquita et al., 2020), reservoir operating rules (de Araújo et al., 2018), reservoir water balance (Feitosa *et al.*, 2021) and reservoir silting (de Araújo *et al.*, 2006, López-Gil *et al.*, 2020).

4 Results

4.1 Spatialised evaporation rate in the reservoirs with AquaSEBS (E_w)

230 Figure 4 shows the spatialised evaporation in the Gavião, Pacoti and Riachão reservoirs. Within-reservoir variability cannot be seen very clearly in the chosen range, which was selected for a better comparison between acquisitions over the years. It is noticeable that over the last decades of monitoring, lower evaporation rates (greenish tones) occur more frequently. The highest evaporation rates are found from 1994 to 2000, which would suggest a declining evaporative pattern in the reservoirs over the last decades. However, we cannot affirm that this apparent decrease represents the reality of the reservoirs,
235 since there are on average only two cloud-free Landsat images per year and there is a degree of uncertainty in the extrapolation of the satellite passage time (instantaneous evaporation) for 24-hour evaporation. From 2000 onwards, one can notice scenes where the evaporation rate is low (about 3 mm day⁻¹), as in the scene obtained in the year 2004. This comes as a result of atypically rainy years in the Ceará state (Medeiros and de Araújo, 2014; Medeiros and Sivapalan, 2020), as the abovementioned year, when the historical average rainfall (800 mm yr⁻¹) was exceeded by over 40% (FUNCEME, 2023). Although the images
240 were obtained in the dry season of each year with low cloudiness, factors such as lower surface temperature and lower relative humidity may have influenced the final product of the algorithm.

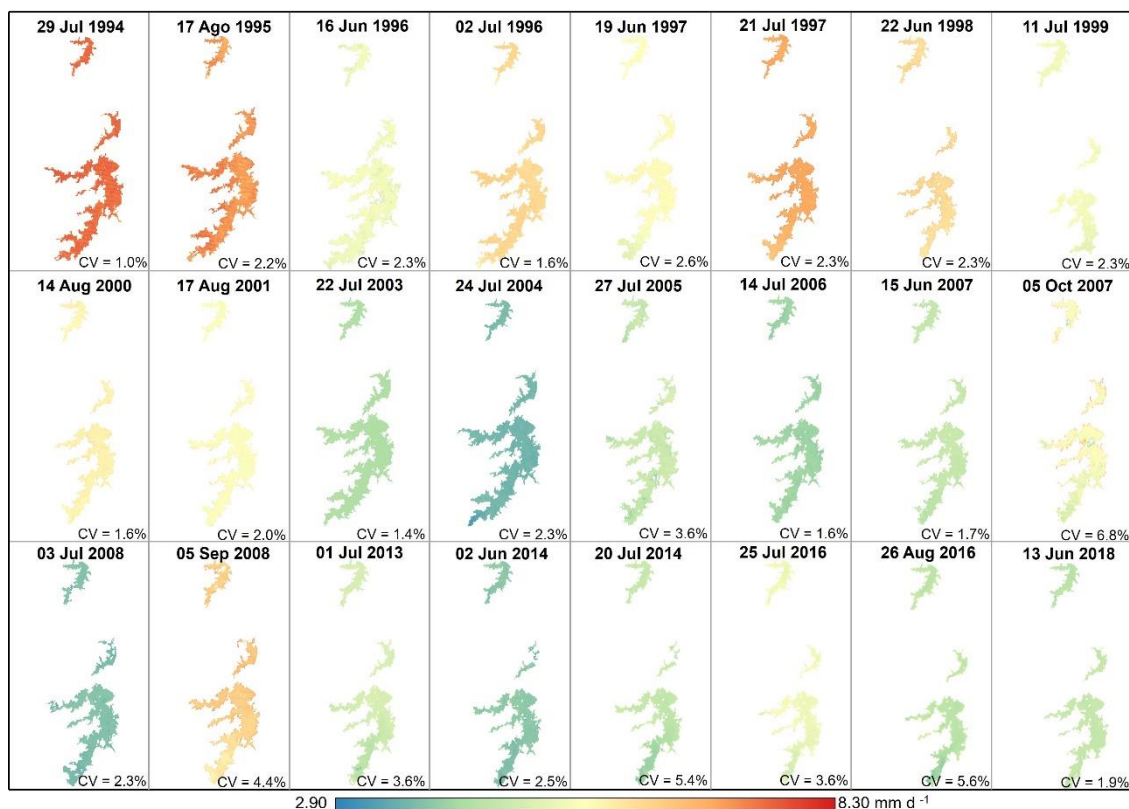


Figure 4: Evaporation rates in the Fortaleza Metropolitan Region reservoirs (Gavião, Riachão and Pacoti) obtained with AquaSEBS algorithm for 24 individual days in the period 1994-2018.

245

Different reservoirs have different evaporation rates due to several drivers, such as depth, surface area and water transparency. The first two factors influences the change in water heat storage and the phase lag between energy and evaporation rate; the latter is directly related to the albedo, which depend on the water quality changes the reflection properties of the surface (Mesquita et al., 2020; McMahon et al., 2016). However, after evaluating the reservoir pixels with AquaSEBS, we observed that the daily evaporation rates and the coefficient of variation (see Figure 4) did not differ substantially, regardless of whether the reservoir evaporation were assumed separately or as a single raster. Thus, we assumed that the reservoirs are subject to the same evaporation rate. Regarding the spatial variability of evaporation within the water bodies, it is necessary to highlight the uncertainty in the result related to the only-water pixels. This is caused by the presence of aquatic plants or exposed soil on some of the banks of the reservoirs, which are captured by the Landsat pixels (spatial resolution = 30 m), thus, hindering the accuracy of the assessment.

255



4.2 Comparison between on-land evaporation (E_L) and remote-sensed evaporation assessment

Table 3 shows the comparison between the on-land (E_L) and on-water (E_w) evaporation rates. In general, the average daily evaporation rates differ by 27%, in which the on-land evaporation rate is constantly higher than the on-water evaporation rate: E_w averages 7.12 mm d⁻¹ against an average E_L of 5.24 mm d⁻¹ (Figure 5). The correction value K_R averages 0.73 (Figure 6). We also examined the data in order to detect a possible correlation of K_R values with the period of the year when evaporation rates were estimated (for example, higher ratios at the end of the dry season). However, no correlation was found between the coefficient and the period of assessment. Most of the highest K_R values (above 0.85) were registered in the first years of monitoring; six of the seven ratios at this threshold are from before 1999. Future investigations may investigate the correlation of this with factors not addressed in this paper, such as features on the satellite sensor, for instance.

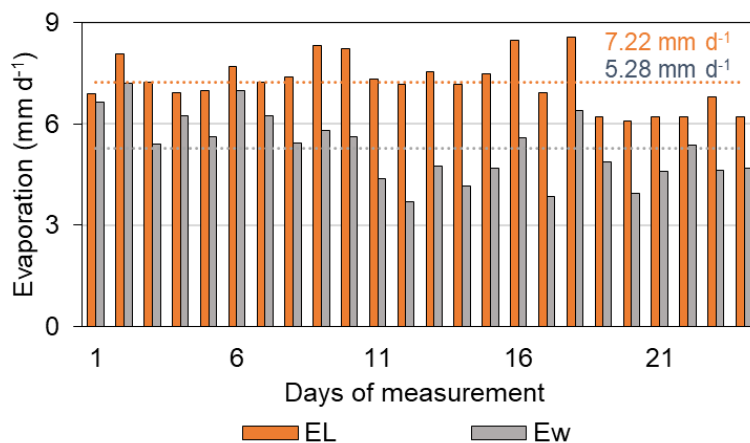
Table 3. Evaporation in Gavião, Riachão and Pacoti reservoirs (1994-2018): comparative results of on-water (E_w) and on-land (E_L) daily rates. The lower part of the table shows statistical parameters. Dates in italic refers to Landsat 8 acquisitions.

n	Date	Pixel count*	E _L (mm d ⁻¹)	E _w (mm d ⁻¹)**	K _R
1	29/07/1994	27350	6.89	6.65	0.96
2	17/08/1995	48980	8.08	7.19	0.89
3	16/06/1996	57108	7.23	5.40	0.75
4	02/07/1996	47735	6.92	6.24	0.90
5	19/06/1997	38887	6.98	5.61	0.80
6	21/07/1997	36370	7.69	6.97	0.91
7	22/06/1998	23277	7.25	6.23	0.86
8	11/07/1999	17344	7.39	5.43	0.73
9	14/08/2000	34668	8.31	5.82	0.70
10	17/08/2001	32373	8.24	5.61	0.68
11	22/07/2003	55487	7.31	4.37	0.60
12	24/07/2004	53372	7.18	3.70	0.52
13	27/07/2005	41088	7.54	4.74	0.63
14	14/07/2006	39100	7.16	4.15	0.58
15	15/06/2007	38071	7.47	4.70	0.63
16	05/10/2007	34419	8.48	5.60	0.66
17	03/07/2008	38744	6.93	3.84	0.55
18	05/09/2008	41943	8.55	6.38	0.75
19	<i>01/07/2013</i>	35519	6.19	4.88	0.79
20	<i>02/06/2014</i>	31122	6.09	3.94	0.65
21	<i>20/07/2014</i>	30688	6.20	4.60	0.74
22	<i>25/07/2016</i>	26976	6.20	5.38	0.87
23	<i>26/08/2016</i>	27823	6.80	4.62	0.68



24	13/06/2018	28585	6.21	4.69	0.75
Average		35934	7.22	5.28	0.73
Median		35945	7.20	5.39	0.74
Min		27350	6.09	3.70	0.52
Max		57108	8.55	7.19	0.96
Std		12183	0.74	0.99	0.12
CV		0.27	0.10	0.19	0.17

270 * Number of reservoir pixels in the raster
 ** Each value refers to the average of the pixels in the three reservoirs



275 **Figure 5: Daily evaporation estimated with the AquaSEBS algorithm (E_w) and calculated based on variables obtained from the INMET station (EL). The analysed period is from 1994 – 2018, 24 days of measurement.**

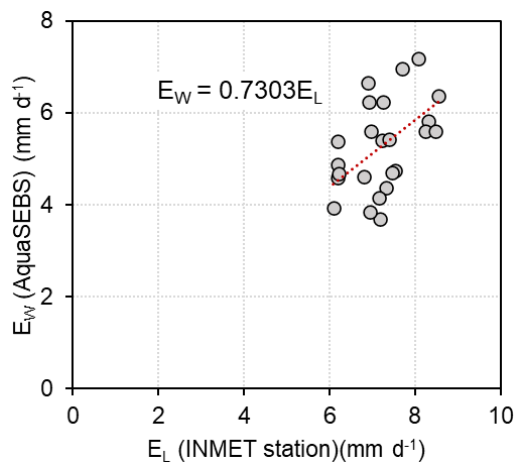


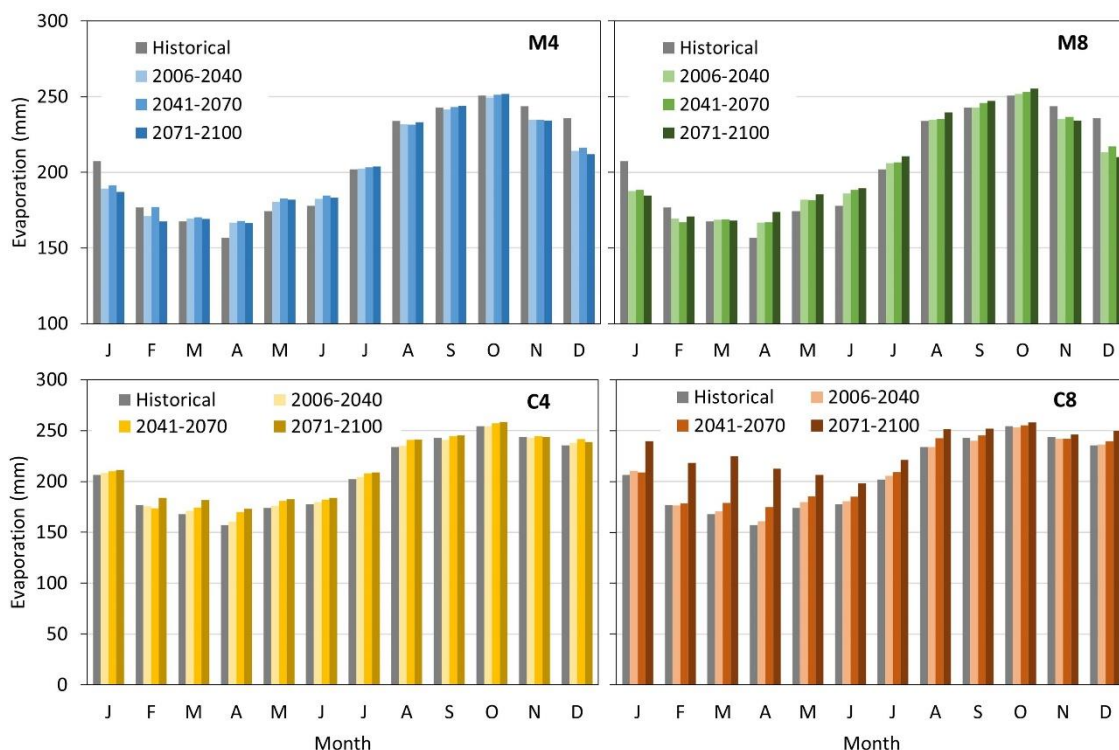
Figure 6: Relationship between daily evaporation estimated with the AquaSEBS algorithm (E_w) and calculated based on variables obtained from the INMET station (EL). The analysed period is from 1994 - 2018.



280 4.3 Evaporation simulation under four climate change scenarios

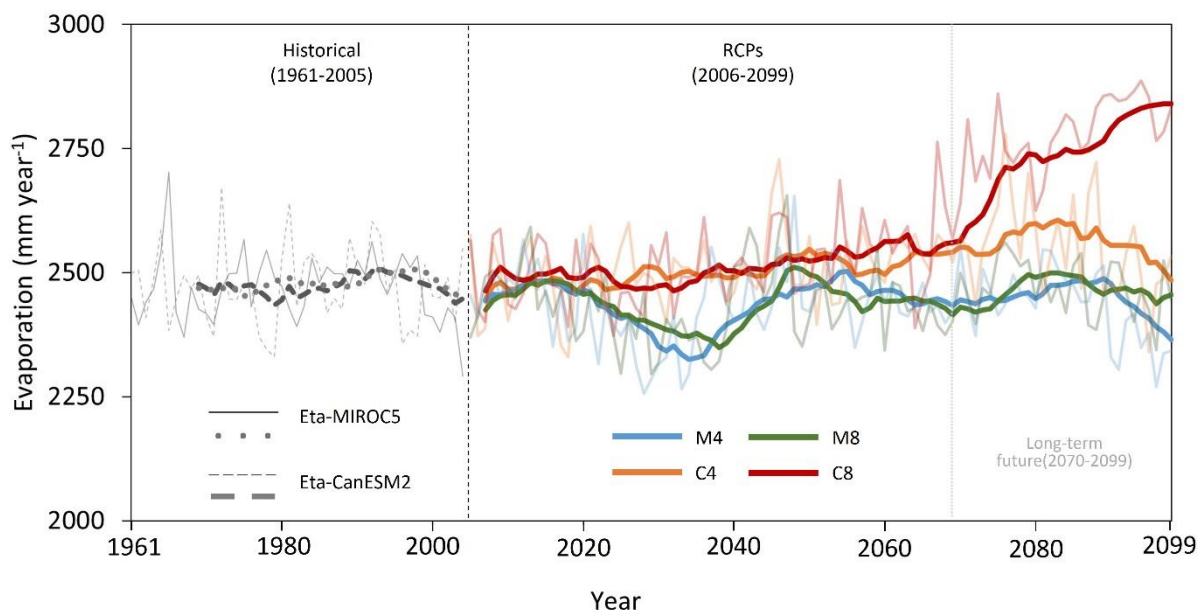
Figure 7 shows the behaviour of monthly evaporation rates for the four temporal slices: historical (1961-2005), near term (2006-2040), midterm (2041-2070), and long term (2071-2099). The two scenarios derived from the Eta-MIROC5 model (M4 and M8) presented similar behaviour, varying only in the magnitude of the evaporation rates. In summary, both scenarios predict a reduction in the evaporative rate in the first two months of the year, stability until the middle of the dry season, and
285 a reduction in the last two months of the year. April was the only month that showed a consistent increase in evaporative rate, 3% and 4% for the scenarios M4 and M8, respectively. The months of November and December show the greatest expected reduction in evaporation, ranging from -3% to -10%, respectively.

The scenarios derived from the Eta-CanESM2 model (C4 and C8) show a possible increase in evaporation rate throughout the whole year. However, the greatest increment is expected in the rainy season for the long-term future (2071-
290 2099) under the C8 scenario. The largest absolute variations are expected in March and April of long-term future (8 and 10% increase respectively). The C4 scenario shows stability for the near future (2006-2040) in the dry (from -1% in September to 1% in December) and in the wet seasons (-1% in February and 2% in March and April). The C8 scenario also shows the largest absolute variations in March and April, but the increase is 34% and 35% respectively, for the long-term future. It is possible that a combination between the reduction in relative humidity and increase in temperature in the rainy season, explains this
295 different behaviour of evaporation between the two seasons (Qin et al., 2021). Moreover, the downscaling done by the regional models for the C4 and C8 scenarios indicate that the wind speed is expected to increase in the rainy season and decrease in the summer season. The decrease in relative humidity occurs systematically throughout the year, but more pronounced in the rainy season.



300 **Figure 7: Scenarios of monthly evaporation rates for the Historical (1961-2005) and RCPs (2006-2099) periods on the Metropolitan Region of Fortaleza. The rates refer to on-water evaporation (E_w).**

Figure 8 shows an overview of the annual evaporation rates for the modelled historical periods and the four climate change scenarios. A distinct pattern of the models is evident if the 10-year average is considered: the scenarios C8 indicates
 305 an upward behaviour, whereas C4, M4 and M8 shows a stabilisation followed by a decrease. From Figure 7 one can depict that there is an increasing behaviour for all scenarios in the beginning of the 2010s. Afterwards, a downward trend is observed for the M4 and M8 scenarios. Except for C8 (which shows a substantial increase), all scenarios tend to maintain the evaporation rate in the long-term future. Over the last decade of simulation (2090s), the M4 scenario presents a more abrupt decrease, while M8 and C4 remain steady.



310 **Figure 8:** Simulated annual on-water evaporation for the Metropolitan Region of Fortaleza. The dashed lines represent the simulated Historical (1961-2005) period, and bold lines refer to the 10-year moving averages.

Table 4 presents the statistical metrics related to the trend analyses of evaporation for all scenarios under the Historical and RCPs experiments. The results indicate no statistically significant variation for the historical simulation of both models (p -value > 0.05). The M8, C4 and C8 scenarios envisage an increase in the evaporation rate of the reservoirs in the period from 2006 to 2099. However, the Mann-Kendall test detected significant variation simulated by Eta-CanESM2 only: +0.40 mm yr⁻¹ for C4 scenario and +4.30 mm yr⁻¹ for the C8. The M4 scenario is the only one that projects a decrease (-0.01 mm yr⁻¹) in evaporation, but with no significant trend.

320 **Table 4.** Mann-Kendall statistics for annual evaporation projected by the regional models for Historical (1961-2005, $n = 45$), and the RCPs (2006-2099, $n = 93$) experiments. Bold numbers are statistically significant (p -value < 0.05). The p -values were determined using a two-sided Kendall tau test (Kendall and Gibbons, 1990).

	Historical		Scenarios			
	Eta-MIROC5	Eta-CanESM2	M4	M8	C4	C8
tau	0.008	0.010	-0.003	0.105	0.192	0.582
p-value	0.945	0.930	0.969	0.136	0.600	< 0.001
Sen's slope (mm yr⁻¹)	0.07	0.04	-0.01	0.42	0.40	4.30

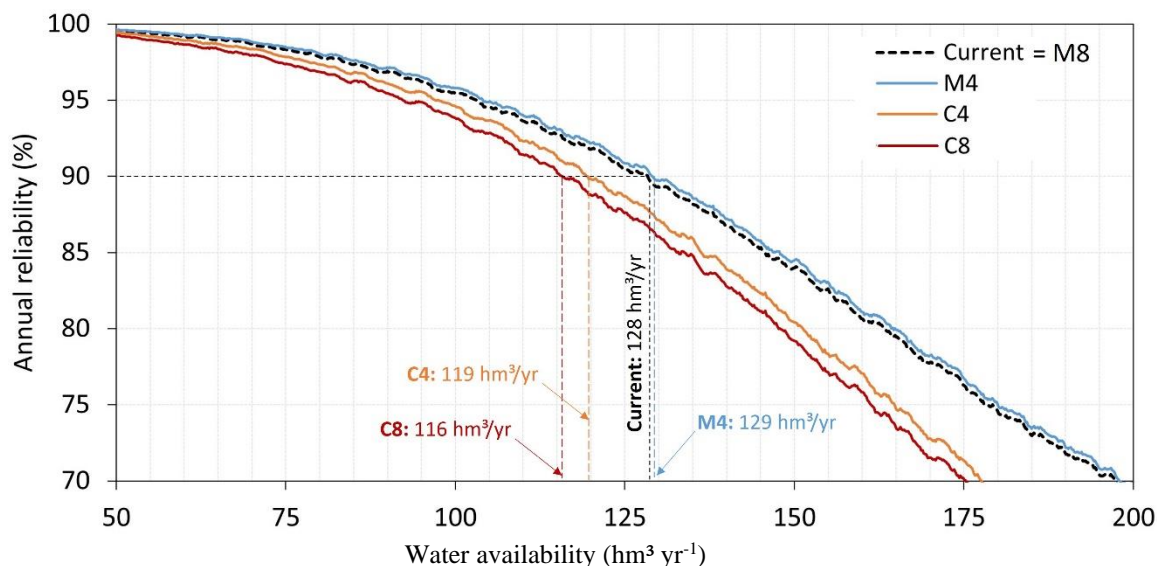
Based on the above findings, we can therefore state that the worst-case scenario in terms of evaporative rate is scenario C8 (+6%) since it increases the evaporative rate in the dry season in the Fortaleza Metropolitan Region. It is worth noting that these rates change when the average annual evaporation, i. e. including both rainy and dry seasons, is considered: -1% under the M4 scenario and +12% under C8 (results not presented?).



4.4 Water availability assessment for the period 2071-2100

330 Figure 9 depicts the relation among water yield with their respective annual reliability for the investigated reservoirs in the long-term future. The dashed line refers to the current water availability of the Gavião-Riachão-Pacoti system, whose water yield with 90% annual reliability (Q_{90}) is $127 \text{ hm}^3 \text{ yr}^{-1}$. For the scenario C4, the Q_{90} is $119 \text{ hm}^3 \text{ yr}^{-1}$, and for C8 it is $116 \text{ hm}^3 \text{ yr}^{-1}$, which consists in reduction of 6% and 9%, respectively. On the other hand, for the scenario M4, the Q_{90} increases to $129 \text{ hm}^3 \text{ yr}^{-1}$, resulting in 1% of increase in the water availability of the reservoir system. Scenario M8 projects no change in the

335 future evaporation rate, hence it is not displayed. It is also noteworthy in Figure 7 that, for higher reliability levels (e.g., 99%), there is less variation in water availability between the scenarios, while for smaller reliability levels (e.g., 75%), the differences become more pronounced. That means that the impact of evaporation is greater in regimes of reduced water reliability.



340 **Figure 9: Water availability as a function of annual reliability level for the Gavião, Riachão and Pacoti reservoirs. Each curve represents a different evaporation rate: current (1961-2005) historical average and four climate change scenarios (M4, M8, C4, and C8) at the end of the 21st Century.**

It is noteworthy in Figure 7 that, although the C8 scenario reports a + 6% change in evaporation rate and the M4 scenario reports -2%, the water availability does not respond linearly to such variations. Table 5 shows the influence of evaporation on water availability for the case of the Fortaleza Metropolitan Region reservoirs. The results indicate that evaporation has a

345 relevant impact on water availability in the region depending on the scenario. Consequently, the reservoir capacity to supply



water with high reliability is reduced. It is relevant to stress that global average elasticity is -0.83, and this value is comparable to siltation impacts observed in reservoirs of the semiarid region (-0.80, as found by de Araújo *et al.*, 2006).

350

Table 5. Elasticity (ϵ) for the current conditions of water availability in the Metropolitan Region of Fortaleza and for the climatic scenarios in the period 2070-2099. The lower part of the table shows the average elasticity.

Scenarios	M4		M8		C4		C8	
	$\Delta E/E^{*1}$	$\Delta Q_{90}/Q^{*90}$	ϵ	$\Delta Q_{90}/Q^{*90}$	ϵ	$\Delta Q_{90}/Q^{*90}$	ϵ	$\Delta Q_{90}/Q^{*90}$
- 0.15	0.099	-0.657	0.092	-0.615	0.052	-0.346	0.023	-0.153
- 0.10	0.072	-0.725	0.059	-0.588	0.015	-0.154	0.000	0.000
- 0.05	0.045	-0.896	0.000	0.000	-0.016	0.317	-0.049	0.984
+ 0.05	-0.024	-0.480	-0.041	-0.813	-0.103	-2.069	-0.143	-2.857
+ 0.10	-0.058	-0.579	-0.085	-0.847	-0.153	-1.532	-0.185	-1.852
+ 0.15	-0.103	-0.690	-0.133	-0.885	-0.196	-1.308	-0.255	-1.699
Average²	-0.014	-0.674	-0.040	-0.627	-0.091	-0.949	-0.126	-1.085

¹ The asterisk refers to the reference values. E^* – M4: 977, M8: 997, C4: 1016, C8: 1052 (all values in mm yr⁻¹). Q^{*90} – M4: 136, M8: 134, C4: 119, C8: 116 (all values in hm³ yr⁻¹)

355 ² The global average is -0.83.

5 Discussion

5.1 Uncertainties addressed in measurement and modelling

In this research, observed evaporation was assessed in two manners: by the Penman (1948) equation with data from a weather station; and by remote sensing. The station, used to correct the bias in simulated data and to calculate evaporation, is 20 km away from the reservoirs. In most cases, meteorological data are obtained from stations distant from the water body, sometimes tens of kilometres away. Feitosa *et al.* (2021) compared measurements on a reservoir (using a floating raft) with a station located on-land in a distance of 30 km. Their results showed overestimation (71%) of open-water evaporation when using data from the on-land station. Mays (2011) warns that neglecting the impact of reservoir evaporation can result in considerable overestimation of water availability and consequent underestimation of the storage capacity required to support water management decisions. Rodrigues *et al.* (2023) found results supporting this statement: Measurements made directly with sensors in a reservoir showed lower averages than historical measurements or previous studies for the same area (Fortaleza Metropolitan Region). The authors recommend monitoring evaporation based on information obtained from meteorological stations as close as possible to the water body when direct measurements cannot be done.

370 Since the late 1990s remote sensing tools contribute to the monitoring of water losses (Bastiaanssen *et al.*, 1998; Bastiaanssen, 2000) however the application to lakes and reservoirs is more recent, and this is particularly true for north-eastern Brazil. Except for the investigation of evaporation trends in Brazilian tropical reservoirs by Rodrigues *et al.* (2021a) and the assessment of spatial variability and impact of riparian vegetation by Rodrigues *et al.* (2021b) there are no applications like



the one in this research for monitoring open water evaporation with remote sensing. In the present study, we also show the
375 limitations of monitoring evaporation during the rainy season: the use of satellite imagery is impractical since cloudiness
impedes visualising the surface. Adding to the limitations in temporal resolution, some reservoirs are rather small and medium
spatial resolution images (such as Landsat, 100 x 100 m thermal band and scheduled every 16 days) may show better results
than lower spatial resolution ones (like MODIS, from 500 m thermal bands and scheduled twice a day). This is due to
“contamination” of water areas with land area information in large pixels. Further, one should take into consideration
380 limitations due to the absence of field data. This is because AquaSEBS, as well as other models for estimating energy balance
and turbulent fluxes (SEBAL, Bastiaanssen et al., 1998; SEBS, Su, 2002), require some information usually acquired on the
ground as inputs (e.g. air pressure, temperature, humidity, or wind speed).

Studies report that remote sensing algorithms have a tendency to underestimate evaporation in high-temperature areas (Gokool
et al., 2017; Rodrigues *et al.*, 2021a), such as tropical-coastal Northeast Brazil. This feature may have influenced the on-water
385 evaporation, assessed with the help of AquaSEBS. It is shown in Table 3 that the pixel count varies. This is mainly driven by
two factors, (i) the presence of clouds and cloud shadow (that were masked out) and (ii) the water level in the reservoirs. The
first factor, however, is more strongly related to the final number of pixels used because the reservoirs are maintained full
(above 80% of the storage capacity) even in the dry season, which affects the spatial representation less than the gaps produced
by the cloudiness.

390 The climate simulations revealed great variations between the regional model outputs and within the historical series of each
model. Indeed, climate models mimic the physical mechanisms of the planet, however, data-based representation is not always
satisfactorily accurate, particularly when dealing with complex hydrological processes such as lake evaporation. There are
external climatic factors such as solar radiation, the Earth's orbit, atmospheric concentrations of greenhouse gases and other
atmospheric factors that increase uncertainty. Besides, there are internal factors in the model system that diminish or amplify
395 the effects and generate a high variability (Kundzewicz et al., 2018).

Chou *et al.* (2014) state that, before using climate models as tools to estimate future climate change impacts, the systematic
errors of current climate simulations need to be estimated in order to assign some degree of confidence to future climate
scenarios. Climate models simulate different future climates which are equally plausible for the same period (in the present
case, up to the end of the 21st century). By using bias correction methods, the aim is to bring model simulations closer to real
400 world measurements over a given reference period (baseline). A bias correction method that is valid for the historical validation
period should then remain valid for future climate change impact studies (Chen *et al.*, 2020). This assumption has been widely
accepted in climate change impact studies (Kundzewicz et al., 2018; Teutschbein and Seibert, 2012; Fiseha et al., 2014). Yet
the performance of bias correction can be affected by climate models with different sensitivities to the real system (Chou *et al.*,
et al., 2014). Regionally, although driven by a single GCM, various downscaling methods may lead to different future climate
405 scenarios (Adachi and Tomita 2020; Kendon *et al.* 2017; Maraun *et al.* 2015; Tang *et al.* 2016). Downscaling regional climate
simulations is another source of uncertainty. While much attention has been paid to the uncertainties of future projections
associated with the choices of GCMs (Moges *et al.* 2021), fewer analyses have quantified the downscaling uncertainty



(Ahmadalipour *et al.* 2018). Generally, it is recommended to use an ensemble of simulations by multiple GCMs and downscaling techniques for reliable regional climate projections (Dibike *et al.* 2017; Pierce *et al.* 2013).

410 A notable feature is the uncertainty intrinsic to the climate models themselves. Both simulated similarly the historical period (Eta-MIROC5 with 16.2% difference from the observed data and Eta-CanESM2 with 16.4%). However, when the RCP experiment starts, the four model-derived scenarios behave in different directions. The high variability found in the simulations is attributed to external climate factors such as solar radiation, Earth orbit, atmospheric concentrations of greenhouse gases, and internal factors in the GCMs themselves (Kundzewicz *et al.*, 2018).

415 Despite the systematic errors inherent in all simulations, the development of regional models for Brazil is essential, as this increases the possibility to better understand the impacts of climate change in various regions, given that it is a country of continental dimensions (8,5 million km²) with climatic, environmental, social, and economic particularities. Our results show that Eta-CanESM2 and Eta-MIROC5 data for Brazil have various biases, which can be originated from the driving GCMs, introduced by the downscaling RCM, and related to uncertainties in observational data. It is expected that such biases, due to

420 the generalised information about the region, are also present in our results, and if the output data are not corrected, any hydrological application will be compromised. Future analyses can be carried out for the study region of this research, such as analysis of the change in the aridity index or the impact of changes in other hydrological processes of relevance for dry regions. The impact on water availability can be reported from two perspectives: first, as a change in reliability for a predefined withdrawal volume and, second, as a change in the available withdrawal volume for a given reliability level (de Araújo *et al.*,

425 2006). For instance, 128 hm³ yr⁻¹ could be taken from the reservoirs system with 90% reliability under the current climate conditions, but only 116 hm³ yr⁻¹ could be withdrawn with the same reliability under scenario C8 conditions in the period from 2071. This reduction in water availability corresponds to a substantial loss of water resources: under the assumption of per capita consumption of 150 L day⁻¹, the difference in water yield would be enough to supply around 200 000 people per year, 6% of the FMR's population.

430 **5.2 Evaporation analysis**

Our findings show two opposite trends for the same study area: one climate model shows an increase in evaporative rate when compared to the historical period and the other shows a decrease. In fact, there are records around the world of positive and negative trends in evaporation. Liu *et al.* (2004) found that the evaporation of 85 Class A pans in China, between 1955 and 2000, had decreased at an average rate of 29.3 mm per decade. Roderick and Farquhar (2004) observed in regions with large

435 industrial centres in Australia that evaporation reduced by an average of 4.3 mm between 1970 and 2002. Similarly, reductions in evaporation were observed in Canada (Burn and Hesch, 2007), India (Chattopadhyay and Hulme, 1997) and Italy (Moonen *et al.*, 2002). On the contrary, the findings of Zhao *et al.* (2022) show an increasing trend of evaporation at global scale by 0.9% per decade for the period 1985 to 2018. Positive trends in reservoir evaporation were also observed in Benin, West Africa (Houngue *et al.*, 2019), Austria (Duethmann and Blösch, 2018), Australia (Helfer *et al.*, 2012; Fuentes *et al.*, 2020), centre-

440 west Brazil (Althoff *et al.*, 2019), Czech Republic (Mozny *et al.*, 2020) and in other parts of the world, generally associated



with countries or regions with low rates of gas-emissions/industrialization (Wang *et al.*, 2014; Miralles *et al.*, 2014). These different trends of increase and decrease in evaporation in various regions of the planet have been called an “evaporation paradox” (Brutsaert and Parlange, 1998).

445 A priori it seems a matter of mere model selection to make important water management decisions in a region sensitive to climate change. Indeed, temperature is rising on a global level (Solomon *et al.*, 2007; Darshana *et al.*, 2013; Qin *et al.*, 2021), and this is expected to be directly related to an increase in evaporation rates. Be that as it may, it should be considered that the historical simulation of both the Eta-CanESM2 and Eta-MIROC5 models was quite similar to what was recorded by the INMET stations (overestimates of 16.2 % and 16.3 %, respectively). Rodrigues *et al.* (2021b) analysed the evaporation trend in Ceará reservoirs for the period 1985 - 2018 using the AquaSEBS model and assessed negative trends (− 0.26 to − 0.08
450 mm/34 years). According to the authors, such behaviour was attributed to the impact of regional air pollution, analogous to the global dimming effect of reduced evaporation in reservoirs located closer to nearby industrial areas (around 2000, according to IPECE, 2017). This causes an increase in the number of clouds and reduces the influence of solar radiation heating on the evaporation of the water body. However, although Fig. 6 shows a similar pattern to the results of the authors op cit, our results do not have sufficient basis to affirm this. Especially when considering the more continuous modelled data, this trend of a
455 reduction in the evaporative rate is not evident.

5.3 Water availability

Campos (2010) states that in Brazil, the annual reliability discharge of 90% is commonly used for water resources planning and can be interpreted as the reference water availability of the reservoir. Recio-Villa *et al.* (2018) also used annual reliability
460 to establish reference water availability, however, they recommend a reliability level of 75% for reservoirs located in a humid tropical climate, which is the case of the region where the reservoirs studied in the present paper are located. Despite this recommendation, we used Q_{90} as a rule for two main reasons: i) the reservoirs of the Metropolitan region of Fortaleza are supplied by a long network of reservoirs located in a semiarid region with water deficit during two thirds of the year and high rainfall uncertainty; ii) the water from these reservoirs is mainly used for industries, agriculture and for the direct supply of
465 about 4 million inhabitants. It should be considered that such a simulated water availability is affected by changes in the evaporation rate. In Ceará, the reservoirs usually suffer a process of reduction in storage capacity mainly due to sediment deposition in the reservoirs (de Araújo *et al.*, 2023) because of erosion; and also due to the high rate of water pollution, mostly caused by eutrophication (Mesquita *et al.*, 2020). Our study highlights another important factor affecting water availability, which is the evaporation rate influenced by climate changes (elasticity concept, as in de Araújo *et al.*, 2006).
470 As stated by Krol *et al.* (2003), climate impacts are not merely an effect of changes in water availability but emerge from the confrontation between availability and societal demands, and also the role these demands play in society. This explains why a study should include not only the physical understanding of climate impacts on the water balance, but also the analysis of



water use, agricultural economy, and societal impacts. This clearly demonstrates that the study of climate change impacts in developing semiarid regions calls for an integrated approach.

475 Besides the uncertainty associated with future water availability, there is substantial uncertainty regarding future water demand (Kundzewicz et al., 2018). The findings of de (de Araújo et al., 2004) indicate that 60 % of the municipalities of the state of Ceará may suffer from long-term water scarcity by 2025. On average, the probability of these municipalities facing a water shortage ranges from 9 % to 20 % annually. Silva *et al.* (2021) analysed climate change impacts and population growth rates in a basin whose sole reservoir provides water to an urban area of 1 million inhabitants in north-eastern Brazil. The rates of

480 change in population growth for the period from 2015 to 2030 varied between 0.9% and 0.8%. Water recycling and more efficient technologies can decrease overall water demand. In fact, the results of the investigation by Rodrigues *et al.* (2020) in a tropical reservoir in northeast Brazil indicated that the investment in building a floating photovoltaic power generation system could reduce water losses due to evaporation by approximately $2.6 \times 10^6 \text{ m}^3 \text{ yr}^{-1}$, enough to supply about 50,000 people, whereas the initial investment in the construction would be fully recovered within eight years. Indeed, cooling techniques for

485 electricity generation are among the most influential climate change mitigating factors affecting future water demand.

6 Conclusions and outlook

Climate simulations made with the regional models Eta-CanESM2 and Eta-MIROC5 showed different trends in the future evaporation of a reservoir network. Similarly, these trends affected regional water availability of the region in opposing

490 patterns. Four scenarios derived from the RMs were evaluated, and from the results, the following conclusions can be drawn: The scenarios derived from the Eta-CanESM2 model (C4 and C8) indicate an increase in dry season evaporative rates: 2% and 6% respectively. The total annual increase, i.e., including both rainy and dry seasons, indicate 12% for the worst-case scenario. Unlike the above scenarios, the ones derived from the Eta-MIROC5 model (M4 and M8) display a decrease in the dry season evaporative rate, -2% in the M4 scenario, and no change in M8. Nevertheless, there is a statistically significant evaporation

495 trend only for the scenarios C4 (+ 0.87 mm yr⁻¹) and C8 (+ 4.30 mm yr⁻¹). Regarding the impact of the simulated evaporation on water availability: For a 90% reliability level, the expected range of change in water availability is -7% to +9%. The scenario C8 envisages the highest reduction in annual water flow while M4 predicts the highest decrease.

It is reasonable to state that both patterns of future evaporation in the reservoirs of the Metropolitan Region of Fortaleza are plausible. To reduce uncertainties in modelling future water availability an adaptive management strategy is recommended, in

500 combination with continuous monitoring of climate change and regional development, as it directly affects water demand. Because model-based projections of climate impact on water resources can be quite divergent, it is necessary to develop adaptations that do not need quantitative projections of changes in hydrological variables, but rather ranges of projected values. Adaptive planning should be based on ensembles and probabilistic approaches from multiple models rather than, for example, a single scenario or a single-value projection. Naturally, improvements on evaporation measurements are needed in order to



505 feed climate models and remote sensing algorithms, which are highly dependent on measured data. Spatialised and continuous field information can improve the simulations of regional models, as they serve as basis for bias correction and ground truth, and thereby increase their reliability. We believe our findings can complement an estimation of water availability, which is especially important during the dry season of the year (June to December) in north-eastern Brazil.

The present research assessed the impact of evaporation from reservoirs on water availability, although the impact of water quality, silting, and increase in per capita consumption should also be taken into consideration in future investigations. It is necessary, therefore, that water management agencies propose adaptation measures for different scenarios, and this study contributes to decision-making aimed at water security during the dry season. Further investigations in densely-populated areas situated in dry regions may find in these results a reference for studies that take into account other variables which were not addressed in our study.

515 **Data availability**

The historical series observed in Ceará can be obtained from <https://bdmep.inmet.gov.br/> in the INMET database. All the CMIP5 RCM outputs are publicly available in the National Institute for Space Research (INPE, Brazil) database, at the INPE Portal “Climate Change in Brazil” and made available on the PROJETA Platform (<https://projeta.cptec.inpe.br>).

Author contributions

520 GP Rodrigues made the computational analysis and prepared the paper. A Brosinsky elaborated additional research ideas and supervised the work. IS Rodrigues and GL Mamede participated in the design, writing and revision of the manuscript. JC de Araújo designed the research approach and supervised the work.

Competing interests

The contact author has declared that neither of the authors has any competing interests.

525 **Disclaimer**

Publisher's note: Copernicus Publications remains neutral with regard to jurisdictional claims in published maps and institutional affiliations.



Acknowledgements

530 The authors acknowledge: (1) funding provided by the Brazilian CAPES (Coordination for the Improvement of Higher
Education Personnel and the German Academic Research Service (DAAD); (2) FUNCAP (Ceará State Foundation for the
Support of Scientific and Technological Development) for the scholarship granted to the first and third authors; (3) COGERH
(Water Resources Management Company of Ceará) for the technical support at the Gavião Reservoir; (4) the University of
Potsdam for the support during Gláuber Rodrigues's staying at the Institute of Environmental Science and Geography; and
535 (5) Gerd Bürger (University of Potsdam), Saskia Förster (Helmholtz Centre, GFZ) and Birgit Heim (Alfred Wegener Institut,
AWI) for the insightful discussion during the preparation of this study.

Financial support

This work was supported by the Coordination for the Improvement of Higher Education Personnel (CAPES) and the German
Academic Research Service (DAAD) by means of the public call no. 23/2019; and the Ceará State Research Foundation
540 (FUNCAP).

References

- Abdelrady, A., Timmermans, J., Vekerdy, Z., and Salama, M. S.: Surface energy balance of fresh and saline waters:
AquaSEBS, *Remote Sens.*, 8, <https://doi.org/10.3390/rs8070583>, 2016.
- Adrian, R., Reilly, C. M. O., Zagarese, H., Baines, S. B., Hessen, D. O., Keller, W., Livingstone, D. M., Sommaruga, R.,
545 Straile, D., Donk, E. Van, Weyhenmeyer, G. A., and Winder, M.: Lakes as sentinels of climate change, *Limnol. Oceanogr.*,
54, 2283–2297, https://doi.org/https://doi.org/10.4319/lo.2009.54.6_part_2.2283, 2009.
- Almagro, A., Oliveira, P.T.S., Rosolem, R., Hagemann, S., Nobre, C.A., 2020. Performance evaluation of Eta/HadGEM2-ES
and Eta/MIROC5 precipitation simulations over Brazil. *Atmos. Res.* <https://doi.org/10.1016/j.atmosres.2020.105053>.
- Althoff, D., Rodrigues, L. N., and Da Silva, D. D.: Evaluating Evaporation Methods for Estimating Small Reservoir Water
550 Surface Evaporation in the Brazilian Savannah, *Water (Switzerland)*, 11, 1–17, <https://doi.org/10.3390/w11091942>, 2019.
- Althoff, D., Rodrigues, L. N., and da Silva, D. D.: Impacts of climate change on the evaporation and availability of water in
small reservoirs in the Brazilian savannah, *Clim. Change*, 159, 215–232, <https://doi.org/10.1007/s10584-020-02656-y>,
2020.
- Bastiaanssen, W. G. M., Menenti, M., Feddes, R. A., and Holtslag, A. A. M.: A remote sensing surface energy balance
555 algorithm for land (SEBAL). 1. Formulation, *J. Hydrol.*, 212–213, 198–212, [https://doi.org/10.1016/S0022-1694\(98\)00253-4](https://doi.org/10.1016/S0022-1694(98)00253-4), 1998.
- Bastiaanssen, W. G. M.: SEBAL-based sensible and latent heat fluxes in the irrigated Gediz Basin, Turkey, *J. Hydrol.*, 229,
87–100, [https://doi.org/10.1016/S0022-1694\(99\)00202-4](https://doi.org/10.1016/S0022-1694(99)00202-4), 2000.



- 560 Bjørnæs C (2013) A guide to representative concentration pathways. Center for International Climate and Environmental Research.
- Brutsaert, W. and Parlange, M. B.: Hydrologic cycle explains the evaporation paradox, *Nature*, 396, 30, <https://doi.org/10.1038/23845>, 1998.
- Burn, D.H., Hesch, N.M., 2007. Trends in evaporation for the Canadian Prairies. *J. Hydrol.* 336 (1-2), 61–73
- 565 Campos, J. N. B. (1996) Dimensionamento de Reservatórios (Reservoir Design, in Portuguese). UFC – Federal University of Ceará, Fortaleza, Brazil.
- Campos, N. J. B.: Modeling the Yield-Evaporation-Spill in the Reservoir Storage Process: The Regulation Triangle Diagram, *Water Resour. Manag.*, 24, 3487–3511, <https://doi.org/10.1007/s11269-010-9616-x>, 2010.
- Chattopadhyay, N. and Hulme, M.: Evaporation and potential evapotranspiration in India under conditions of recent and future climate change, *Agric. For. Meteorol.*, 87, 55–73, [https://doi.org/10.1016/S0168-1923\(97\)00006-3](https://doi.org/10.1016/S0168-1923(97)00006-3), 1997.
- 570 Chou, S. C., Lyra, A., Mourão, C., Dereczynski, C., Pilotto, I., Gomes, J., Bustamante, J., Tavares, P., Silva, A., Rodrigues, D., Campos, D., Chagas, D., Sueiro, G., Siqueira, G., Nobre, P., and Marengo, J.: Evaluation of the Eta Simulations Nested in Three Global Climate Models, *Am. J. Clim. Chang.*, 03, 438–454, <https://doi.org/10.4236/ajcc.2014.35039>, 2014.
- Chylek, P., Li, J., Dubey, M.K., Wang, M., Lesins, G., 2011. Observed and model simulated 20th century Arctic temperature variability: canadian earth system model CanESM2. *Atmos. Chem. Phys.* 11, 22893–22907.
- 575 Cui, X., Guo, X., Wang, Y., Wang, X., Zhu, W., Shi, J., Lin, C., and Gao, X.: Application of remote sensing to water environmental processes under a changing climate, *J. Hydrol.*, 574, 892–902, <https://doi.org/10.1016/j.jhydrol.2019.04.078>, 2019.
- Darshana D, Pandey A, Pandey RP. Analysing Trends in reference evapotranspiration and weather variables in the Tons River basin in central India. *Stochastic Environmental Research and Risk Assess- ment.* 2013; 27(6): 1407–1421
- 580 de Araújo, J. C. and Piedra, J. I. G.: Comparative hydrology: analysis of a semiarid and a humid tropical watershed, *Hydrol. Process.*, 23, 1169–1178, <https://doi.org/10.1002/hyp.7232>, 2009.
- de Araújo, J. C., Döll, P., Güntner, A., Krol, M., Abreu, C. B. R., Hauschild, M., and Mendiondo, E. M.: Water scarcity under scenarios for global climate change and regional development in semiarid northeastern brazil, *Water Int.*, 29, 209–220, <https://doi.org/10.1080/02508060408691770>, 2004.
- 585 de Araújo, J. C., Güntner, A., and Bronstert, A.: Loss of reservoir volume by sediment deposition and its impact on water availability in semiarid Brazil, *Hydrol. Sci. J.*, 51, 157–170, <https://doi.org/10.1623/hysj.51.1.157>, 2006.
- de Araújo, J. C., Mamede, G. L., and de Lima, B. P.: Hydrological guidelines for reservoir operation to enhance water governance: Application to the Brazilian Semiarid region, *Water (Switzerland)*, 10, <https://doi.org/10.3390/w10111628>, 2018.
- 590 Duethmann, D., Blöschl, G., 2018. Why has catchment evaporation increased in the past 40 years? A data-based study in Austria. *Hydrol. Earth Syst. Sci.* 22 (10).



- Feitosa, G. P., de Araújo, J. C., and Barros, M. U. G.: Different methods for measuring evaporation in a tropical reservoir: The case of the gavião reservoir in the state of Ceará, *Rev. Caatinga*, 34, 410–421, <https://doi.org/10.1590/1983-21252021v34n217rc>, 2021.
- 595 Fiseha, B. M., Setegn, S. G., Melesse, A. M., Volpi, E., and Fiori, A.: Impact of Climate Change on the Hydrology of Upper Tiber River Basin Using Bias Corrected Regional Climate Model, *Water Resour. Manag.*, 28, 1327–1343, <https://doi.org/10.1007/s11269-014-0546-x>, 2014.
- Fuentes, I., van Ogtrop, F., Vervoort, R.W., 2020. Long-term surface water trends and relationship with open water evaporation losses in the Namoi catchment. Australia. *Journal of Hydrology* 584, 124714.
600 <https://doi.org/10.1016/j.jhydrol.2020.124714>
- Gokool, S., Jarman, C., Riddell, E., Swemmer, A., Lerm, R., Chetty, K.T., 2017. Quantifying riparian total evaporation along the Groot Letaba River: A comparison between infilled and spatially downscaled satellite derived total evaporation estimates. *J. Arid Environ.* 147, 114–124.
- Graham, L., Hagemann, S., Jaun, S., Beniston, M., 2007b. On interpreting hydrological change from regional climate models.
605 *Clim. Change* 81, 97–122. [http:// dx.doi.org/10.1007/s10584-006-9217-0](http://dx.doi.org/10.1007/s10584-006-9217-0).
- Helfer, F., Lemckert, C., Zhang, H., 2012. Impacts of climate change on temperature and evaporation from a large reservoir in Australia. *J. Hydrol.* 475, 365–378.
- Hounguè, R., Lawin, A.E., Moumouni, S., Afouda, A.A., 2019. Change in Climate Extremes and Pan Evaporation Influencing Factors over Ou´em´e Delta in Benin. *Climate* 7 (1), 2.
- 610 IBGE, 2022. Estados: População. Instituto Brasileiro de Geografia, Rio de Janeiro (Last access: 06 July 2023). <https://censo2022.ibge.gov.br>
- Instituto Nacional de Meteorologia – INMET, 2019. Normais Climatológicas do Brasil. <http://www.inmet.gov.br/projetos/rede/pesquisa/inicio.php> Accessed: 16 December 2022.
- IPCC, 2014. Climate Change 2014: Synthesis Report. Contribution of Working Groups I, II and III to the Fifth Assessment Report of the Intergovernmental Panel on Climate Change. IPCC, Geneva, Switzerland, pp. 151
615
- Kendall, M., Gibbons, J.D., 1990. Rank Correlation Methods. Oxford University Press, Oxford.
- Kendall, M.G., 1975. Rank Correlation Measures. Charles Griffin, London.
- Kendon, E.J., et al., 2017. Do convection-permitting regional climate models improve projections of future precipitation change? *Bull. Am. Meteorol. Soc.* 98 (1), 79–93.
- 620 Konapala, G., Mishra, A. K., Wada, Y., and Mann, M. E.: Climate change will affect global water availability through compounding changes in seasonal precipitation and evaporation, *Nat. Commun.*, 11, 1–10, <https://doi.org/10.1038/s41467-020-16757-w>, 2020.
- Kundzewicz, Z. W., Krysanova, V., Benestad, R. E., Hov, Piniewski, M., and Otto, I. M.: Uncertainty in climate change impacts on water resources, *Environ. Sci. Policy*, 79, 1–8, <https://doi.org/10.1016/j.envsci.2017.10.008>, 2018.



- 625 Liu, B., Xu, M., Henderson, M., Gong, W., 2004. A spatial analysis of pan evaporation trends in China, 1955–2000. *Journal of Geophysical Research: Atmospheres* 109 (D15).
- Lyra, A., Tavares, P., Chou, S. C., Sueiro, G., Dereczynski, C., Sondermann, M., Silva, A., Marengo, J., and Giarolla, A.: Climate change projections over three metropolitan regions in Southeast Brazil using the non-hydrostatic Eta regional climate model at 5-km resolution, *Theor. Appl. Climatol.*, 132, 663–682, <https://doi.org/10.1007/s00704-017-2067-z>, 2018.
- 630 Malveira, V.T.C., de Araújo, J.C., Güntner, A., 2012. Hydrological impact of a high- density reservoir network in semiarid northeastern Brazil. *J. Hydrol. Eng.* 17 (1), 109–117
- Mamede, G.L., Araújo, N.A., Schneider, C.M., de Araújo, J.C., Herrmann, H.J., 2012. Overspill avalanching in a dense reservoir network. *Proc. Natl. Acad. Sci.* 109 (19), 7191–7195.
- Mann, H.B., 1945. Nonparametric tests against trend. *Econometrica* 13 (3), 245. <https://doi.org/10.2307/1907187>
- 635 Marengo JA, Jones R, Alvesa LM, Valverde MC. 2009. Future change of temperature and precipitation extremes in South America as derived from the PRECIS regional climate modeling system. *Int J Climatol* 29:2241–2255
- Marengo, J. A., Alves, L. M., Alvala, R. C. S., Cunha, A. P., Brito, S., and Moraes, O. L. L.: Climatic characteristics of the 2010-2016 drought in the semiarid Northeast Brazil region, *An. Acad. Bras. Cienc.*, 90, 1973–1985, <https://doi.org/10.1590/0001-3765201720170206>, 2017.
- 640 Marengo, J. A., Galdos, M. V., Challinor, A., Cunha, A. P., Marin, F. R., Vianna, M. dos S., Alvala, R. C. S., Alves, L. M., Moraes, O. L., and Bender, F.: Drought in Northeast Brazil: A review of agricultural and policy adaptation options for food security, *Clim. Resil. Sustain.*, 1, 1–20, <https://doi.org/10.1002/cli2.17>, 2022.
- McMahon, T. A. & Mein, R. G. (1986) *River and Reservoir Yield*. Water Resources Publications, Littleton, Colorado, USA.
- McMahon, T. A., Finlayson, B. L., and Peel, M. C.: Historical developments of models for estimating evaporation using standard meteorological data, *Wires Water*, 3, 788–818, <https://doi.org/10.1002/wat2.1172>, 2016.
- 645 Medeiros, P. H. A. and de Araújo, J. C.: Temporal variability of rainfall in a semiarid environment in Brazil and its effect on sediment transport processes, *J. Soils Sediments*, 14, 1216–1223, <https://doi.org/10.1007/s11368-013-0809-9>, 2014.
- Mesinger F, Chou SC, Gomes JL et al (2012) An upgraded version of the Eta model. *Meteorog Atmos Phys* 116: 63–79. <https://doi.org/10.1007/s00703-012-0182-z>
- 650 Mesquita, J. B. de F., Lima Neto, I. E., Raabe, A., and de Araújo, J. C.: The influence of hydroclimatic conditions and water quality on evaporation rates of a tropical lake, *J. Hydrol.*, 590, 125456, <https://doi.org/10.1016/j.jhydrol.2020.125456>, 2020.
- Minville M, Brissette F, Leconte R (2010) Impacts and uncertainty of climate change on water resource management of the Peribonka River System (Canada). *J Water Resour Plan Manag* 136:376–385. [https://doi.org/10.1061/\(ASCE\)WR.1943-5452.0000041](https://doi.org/10.1061/(ASCE)WR.1943-5452.0000041)
- 655 Miralles, D.G., van den Berg, M.J., Gash, J.H., Parinussa, R.M., de Jeu, R.A.M., Beck, H. E., Holmes, T.R.H., Jiménez, C., Verhoest, N.E.C., Dorigo, W.A., Teuling, A.J., Johannes Dolman, A., 2014. El Niño–La Niña cycle and recent trends in continental evaporation. *Nat. Clim. Change* 4 (2), 122–126



- 660 Moonen, A. C., Ercoli, L., Mariotti, M., and Masoni, A. (2002). Climate change in Italy indicated by agrometeorological indices over 122 years. *Agricultural and Forest Meteorology*, 111(1), 13–27
- Mozny, M., Trnka, M., Vlach, V., Vizina, A., Potopova, V., Zahradnicek, P., Stepanek, P., Hajkova, L., Staponites, L., Zalud, Z., 2020. Past (1971–2018) and future (2021–2100) pan evaporation rates in the Czech Republic. *J. Hydrol.* 590, 125390. <https://doi.org/10.1016/j.jhydrol.2020.125390>.
- 665 Navarro-Racines, C., Tarapues, J., Thornton, P., Jarvis, A., and Ramirez-Villegas, J.: High-resolution and bias-corrected CMIP5 projections for climate change impact assessments, *Sci. Data*, 7, 1–14, <https://doi.org/10.1038/s41597-019-0343-8>, 2020.
- Oliveira, P. T., Santos e Silva, C. M., and Lima, K. C.: Climatology and trend analysis of extreme precipitation in subregions of Northeast Brazil, *Theor. Appl. Climatol.*, 130, 77–90, <https://doi.org/10.1007/s00704-016-1865-z>, 2017.
- Penman, H. L.: Evaporation: An introductory survey, *Neth. J. Agr. Sci.*, 4, 9–29, 1956.
- 670 Penman, H. L.: Natural evaporation from open water, bare soil and grass, *Proc. R. Soc.*, 193, 120–145, <https://doi.org/https://doi.org/10.1098/rspa.1948.0037>, 1948.
- Peter, S.J., de Araújo, J.C., Araújo, N.A., Herrmann, H.J., 2014. Flood avalanches in a semiarid basin with a dense reservoir network. *J. Hydrol.* 512, 408–420.
- Qin, M., Zhang, Y., Wan, S., Yue, Y., Cheng, Y., and Zhang, B.: Impact of climate change on “evaporation paradox” in province of Jiangsu in southeastern China, *PLoS One*, 16, 1–26, <https://doi.org/10.1371/journal.pone.0247278>, 2021.
- Roderick, M.L., Farquhar, G.D., 2004. Changes in Australian pan evaporation from 1970 to 2002. *International Journal of Climatology: A Journal of the Royal Meteorological Society* 24 (9), 1077–1090.
- Rodrigues, I. S., Costa, C. A. G., Lima Neto, I. E., and Hopkinson, C.: Trends of evaporation in Brazilian tropical reservoirs using remote sensing, *J. Hydrol.*, 598, <https://doi.org/10.1016/j.jhydrol.2021.126473>, 2021b.
- 680 Rodrigues, I. S., Costa, C. A. G., Raabe, A., Medeiros, P. H. A., and de Araújo, J. C.: Evaporation in Brazilian dryland reservoirs: Spatial variability and impact of riparian vegetation, *Sci. Total Environ.*, 797, 149059, <https://doi.org/10.1016/j.scitotenv.2021.149059>, 2021a.
- Rosenzweig, C., et al., 2007. Assessment of observed changes and responses in natural and managed systems. In: M.L. Parry, et al., eds. *Climate change 2007: impacts, adaptation and vulnerability. Contribution of Working Group II to the Fourth Assessment Report of the Intergovernmental Panel on Climate Change*. Cambridge: Cambridge University Press.
- 685 Solomon, S., Qin, D., Manning, M. (Eds.), 2007. *Contribution of Working Group I to the Fourth Assessment Report of the Intergovernmental Panel on Climate Change*. Cambridge University Press.
- Su, Z.: The Surface Energy Balance System (SEBS) for estimation of turbulent heat fluxes, *Hydrol. Earth Syst. Sci.*, 6, 85–99, 2002.
- 690 Teutschbein, C. and Seibert, J.: Bias correction of regional climate model simulations for hydrological climate-change impact studies: Review and evaluation of different methods, *J. Hydrol.*, 456–457, 12–29, <https://doi.org/10.1016/j.jhydrol.2012.05.052>, 2012.



- Wang, W., Xiao, W., Cao, C., Gao, Z., Hu, Z., Liu, S., Shen, S., Wang, L., Xiao, Q., Xu, J., Yang, D., Lee, X., 2014. Temporal and spatial variations in radiation and energy balance across a large freshwater lake in China. *J. Hydrol.* 511, 811–824.
- 695 Watanabe M, Suziki T, O’ishi R, Komuro Y, Watanabe S, Emori S, Takemura T, Chikira M, Ogura T, Sekiguchi M, Takata K, Yamazaki D, Yokohata T, Nozawa T, Hasumi H, Tatebe H, Kimoto M. 2010. Improved climate simulation by MIROC5: mean states, variability, and climate sensitivity. *J. Clim.* 23(23): 6312–6335. <https://doi.org/10.1175/2010JCLI3679.1>.
- Zhang, S., Foerster, S., Medeiros, P., de Araújo, J. C., Duan, Z., Bronstert, A., and Waske, B.: Mapping regional surface water volume variation in reservoirs in northeastern Brazil during 2009–2017 using high-resolution satellite images, *Sci. Total*
- 700 *Environ.*, 789, <https://doi.org/10.1016/j.scitotenv.2021.147711>, 2021.